J|A|C|S
ARTICLES

Published on Web 08/22/2008

The Mechanism of Long-Range Exciton Diffusion in a Nematically Organized Porphyrin Layer

Annemarie Huijser,[†,§] Tom J. Savenije,[†] Stefan C. J. Meskers,[‡] Martien J. W. Vermeulen,[†] and Laurens D. A. Siebbeles*[,†]

Opto-Electronic Materials Section, DelftChemTech, Faculty of Applied Sciences, Delft University of Technology, Julianalaan 136, 2628 BL Delft, The Netherlands, and Molecular Materials and Nanosystems, Eindhoven University of Technology, PO Box 513, 5600 MB Eindhoven, The Netherlands

Received May 20, 2008; E-mail: L.D.A.Siebbeles@tudelft.nl

Abstract: The exciton diffusion length in a nematically organized *meso*-tetra(4-*n*-butylphenyl)porphyrin (TnBuPP) layer was found to exceed 40 nm at a temperature of 90 K and to be equal to 22 ± 3 nm at 300 K. The exciton diffusion coefficient decreases from $\geq 3.1 \times 10^{-6}$ m^2/s at 90 K to $(2.5 \pm 0.5) \times 10^{-7}$ m^2/s at 300 K. This thermal deactivation is attributed to exciton motion via a band mechanism. The motion of an exciton is not limited by polaronic effects; that is, the deformation of the atomic lattice around the exciton. The absence of polaronic self-trapping implies that the exciton diffusion coefficient can be enhanced by improvement of structural order and rigidity of the material.

I. Introduction

Energy transfer via motion of electronic excited states in molecular materials plays an important role in photosynthetic systems and is a key process in molecule-based photovoltaics and sensors.[1−7] In these systems absorption of a photon brings a molecule into an electronically excited state, which is referred to as an exciton. The exciton needs to diffuse to an active site where its energy can be utilized. In photovoltaics this involves conversion into electrical energy by dissociation of the exciton into free charges, while in molecular sensing systems the exciton decays by fluorescence at an acceptor site. The efficiency of these processes is to a large extent determined by the distance over which an exciton can move before it decays within its lifetime. The exciton diffusion length is defined as

$$\Lambda_E = \sqrt{D_E \tau_E} \quad (1)$$

with D_E the diffusion coefficient and τ_E the exciton lifetime before (non)radiative decay. To realize exciton motion over long distances, fundamental insights into the factors that govern these parameters are essential.

In most molecular materials the exciton diffusion length is at most a few nanometers.[8,9] For conjugated polymers the exciton diffusion length, as defined in eq (1) is typically 5−8 nm[10−13] with the exception of a ladder-type polymer for which an exciton diffusion length of 14 nm has been reported.[14] Interestingly, values of Λ_E in the order of tens of nanometers have been realized for some porphyrin and phthalocyanine derivatives.[15−22] It has recently been shown, that self-assembly of porphyrin derivatives can yield homeotropically aligned structures in which π-stacked columns can provide pathways

† Delft University of Technology.
‡ Eindhoven University of Technology.
§ Present address: Department of Chemical Physics, Lund University, Box 124, S-22100 Lund, Sweden.

(1) van Grondelle, R.; Novoderezhkin, V. I. *Phys. Chem. Chem. Phys.* **2006**, *8*, 793–807.
(2) van Amerongen, H.; Valkunas, L.; van Grondelle, R., *Photosynthetic Excitons*; World Scientific: Singapore, 2000.
(3) Yang, F.; Shtein, M.; Forrest, S. R. *Nat. Mater.* **2005**, *4*, 37–41.
(4) Mayer, A. C.; Scully, S. R.; Hardin, B. E.; Rowell, R. W.; McGehee, M. *Mater. Today* **2007**, *10*, 28–33.
(5) Zhang, C. Y.; Yeh, H. C.; Kuroki, M. T.; Wang, T. H. *Nat. Mater.* **2005**, *4*, 826–831.
(6) Günes, S.; Neugebauer, H.; Sariciftci, N. S. *Chem. Rev.* **2007**, *107*, 1324–1338.
(7) Scholes, G. D.; Rumbles, G. *Nat. Mater.* **2006**, *5*, 683–696.
(8) Kerp, H. R.; Donker, H.; Koehorst, R. B. M.; Schaafsma, T. J.; van Faassen, E. E. *Chem. Phys. Lett.* **1998**, *298*, 302–308.
(9) Kroeze, J. E.; Savenije, T. J.; Warman, J. M. *J. Photochem. Photobiol. A* **2002**, *148*, 49–55.
(10) Theander, M.; Yartsev, A.; Zigmantas, D.; Sundstrom, V.; Mammo, W.; Andersson, M. R.; Inganas, M. R. *Phys. Rev. B* **2000**, *61*, 12957.
(11) Markov, D. E.; Hummelen, J. C.; Blom, P. W. M. *Phys. Rev. B* **2005**, *72*, 045216.
(12) Lewis, A. J.; Ruseckas, A.; Gaudin, O. P. M.; Webster, G. R.; Burn, P. L.; Samuel, I. D. W. *Org. Elem.* **2006**, *7*, 452–456.
(13) Gulbinas, V.; Mineviciute, I.; Hertel, D.; Wellander, R.; Yartsev, A.; Sundstrom, V. *J. Chem. Phys.* **2007**, *127*, 144907.
(14) Haugeneder, A.; Neges, M.; Kallinger, C.; Spirkl, W.; Lemmer, U.; Feldmann, J.; Scherf, U.; Harth, E.; Gugel, A.; Mullen, K. *Phys. Rev. B* **1999**, *59*, 15346.
(15) Peumans, P.; Uchida, S.; Forrest, S. R. *Nature* **2003**, *425*, 158–162.
(16) Peumans, P.; Forrest, S. R. *Appl. Phys. Lett.* **2001**, *79*, 126–128.
(17) Peumans, P.; Yakimov, A.; Forrest, S. R. *J. Appl. Phys.* **2003**, *93*, 3693–3723.
(18) Stubinger, T.; Brutting, W. *J. Appl. Phys.* **2001**, *90*, 3632–3641.
(19) Kroeze, J. E.; Savenije, T. J.; Warman, J. M. *Adv. Mater.* **2002**, *14*, 1760–1763.
(20) Donker, H.; van Hoek, A.; van Schaik, W.; Koehorst, R. B. M.; Yatskou, M. M.; Schaafsma, T. J. *J. Phys. Chem. B* **2005**, *109*, 17038–17046.
(21) Huijser, A.; Savenije, T. J.; Kotlewski, A.; Picken, S. J.; Siebbeles, L. D. A. *Adv. Mater.* **2006**, *18*, 2234–2239.
(22) Huijser, A.; Suijkerbuijk, B. M. J. M.; Klein Gebbink, R. J. M.; Savenije, T. J.; Siebbeles, L. D. A. *J. Am. Chem. Soc.* **2008**, *130*, 2485–2492.

10.1021/ja803753y CCC: $40.75

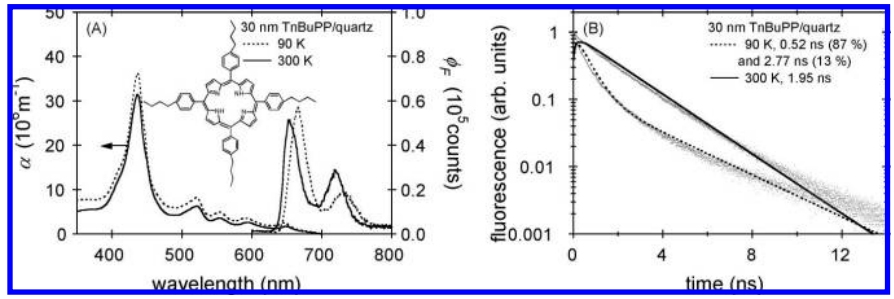

Figure 1. (A) Optical absorption coefficient and fluorescence spectrum for TnBuPP on quartz at 90 K (dashed) and 300 K (solid). The inset shows the chemical structure of TnBuPP. (B) Fluorescence decay of TnBuPP on quartz at 90 and 300 K recorded after excitation at 405 nm and detected at the wavelength for which fluorescence is maximum. Fits of a biexponential (90 K) or monoexponential (300 K) function convoluted with the instrumental response function to the fluorescence decays and the lifetimes are included.

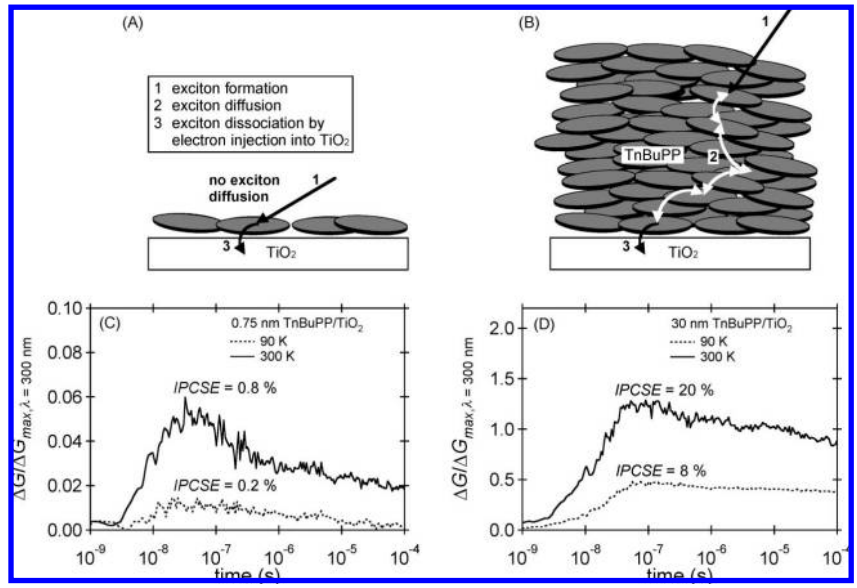

Figure 2. (A) Schematic representation of exciton formation by photon absorption (1) and interfacial exciton dissociation (3) in a thin 0.75 nm layer of TnBuPP on TiO_2. (B) In a 30 nm thick TnBuPP layer excitons must diffuse (2) to reach the interface with TiO_2. Panels C and D show the photoconductance transients at 90 K (dashed) and 300 K (solid) on excitation from the side of the TiO_2 substrate at 430 nm with 2×10^{11} photons/cm^2 per pulse, normalized to ΔG_{max} obtained on excitation at 300 nm with 5×10^{10} photons/cm^2 per pulse.

for charge or exciton transport.[23,24] The present work involves a study of the mechanism of exciton motion in nematically organized layers of *meso*-tetra(4-*n*-butylphenyl)porphyrin (TnBuPP) molecules (see the inset of Figure 1A for the chemical structure of TnBuPP and Figure 2B for the molecular organization). This material is of particular interest, since according to previous results the exciton diffusion length is longer than 12 nm.[21] The aim of the present work is to determine the actual value of Λ_E and the magnitude of the exciton diffusion coefficient and to provide insight into the mechanism of exciton motion in TnBuPP.

Two limiting cases for the mechanism of exciton motion can be distinguished, depending on the strength of the interaction of an exciton with the atomic nuclei in the material; that is, the exciton−phonon coupling. In the first case of strong exciton−phonon coupling, an exciton induces a deformation of the atomic lattice around itself to form a so-called polaronic exciton. Exciton diffusion then occurs via thermally activated hopping between localized states. This is the basis of the commonly used Förster model for energy transfer.[25,26] Thermally activated exciton diffusion has been reported for the conjugated polymer poly(*p*-phenylene vinylene) (PPV).[27] The hopping rate is thermally activated, since for each hop the atomic lattice must reorganize so that the exciton energies at the initial and final molecular sites become equal and resonance energy transfer can take place. The rate of exciton transfer between molecules is analogous to that for polaronic hopping of charge carriers.[28] In the classical limit for which the thermal energy, k_BT, exceeds the energy of the relevant molecular vibrational quanta, the exciton hopping rate can be expressed as[25,26]

$$w = \frac{2\pi|J|^2}{\hbar}\sqrt{\frac{1}{4\pi E_s k_B T}}\, e^{-E_s/4k_BT} \qquad (2)$$

where E_s is the Stokes shift between the energy for photoabsorption and emission, J is the electronic coupling for exciton

(23) Zhou, X.; Kang, S. W.; Kumar, S.; Kulkarni, R. R.; Cheng, S. Z. D.; Li, Q. *Chem. Mater.* **2008**, *20*, 3551–3553.
(24) Li, L.; Kang, S. W.; Harden, J.; Sun, Q. Z., X.; Dai, L.; Jakli, A.; Kumar, S.; Li, Q. *Liq. Cryst.* **2008**, *35*, 233–239.
(25) Markvart, T.; Greef, R. *J. Chem. Phys.* **2004**, *121*, 6401–6405.
(26) May, V.; Kühn, O. *Charge and Energy Transfer Dynamics in Molecular Systems*; Wiley-VCH: Berlin, 2004.
(27) Bjorklund, T. G.; Lim, S.; Bardeen, C. J. *J. Phys. Chem. B* **2001**, *105*, 11970–11977.
(28) Grozema, F. C.; Siebbeles, L. D. A. *Int. Rev. Phys. Chem.* **2008**, *27*, 87–138.

transfer, $\hbar$ is Planck's constant divided by 2π, k_B is the Boltzmann constant, and T is the temperature. The exciton diffusion coefficient is equal to

$$D = wa^2 \tag{3}$$

where a is the distance between the initial and final molecular sites. Note, that it has been assumed in eqs 2 and 3 that the energies of the exciton and the electronic couplings are the same for all molecular sites. This assumption implies that the Stokes shift in eq 2 is entirely due to the structural deformation of the atomic lattice around the exciton and is not affected by energetic relaxation due to dispersive motion of the exciton in a disordered energy landscape, which gives rise to so-called spectral diffusion. If this Stokes shift largely exceeds k_BT, the temperature dependence of the hopping rate in eq 2 is dominated by the exponential factor and the diffusion coefficient is thermally activated. In case the energy of the vibrational quanta is larger than k_BT the classical limit of eq 2 is no longer valid and the vibrations must be treated quantum mechanically. Analogous to the rate in eq 2, also in this case the hopping rate is thermally activated.[28]

In the second opposite case of weak exciton−phonon coupling, the exciton does not induce a lattice distortion around itself. Exciton motion can now be described by a bandlike mechanism. The nonpolaronic exciton diffusion is affected by time-dependent fluctuations in the energy of an exciton at a molecule (site energy, ε) and in the electronic couplings (J) between the molecules. The theoretical models to describe exciton motion are analogous to the tight-binding models for motion of delocalized charges in weakly disordered materials, discussed in ref 28. Haken, Strobl, and Reineker[29,30] have provided an analytical expression for the exciton diffusion coefficient for the case of white-noise-like uncorrelated fluctuations in the site energies, $\varepsilon_{tot}(t) = \varepsilon + \delta\varepsilon(t)$, and nearest-neighbor electronic couplings, $J_{tot}(t) = J + \delta J(t)$, with t being the time. The fluctuations have zero mean value and the second moments of the fluctuations are $\langle \delta\varepsilon(t)\ \delta\varepsilon(t')\rangle = 2\gamma_0\hbar\ \delta(t\text{-}t')$ and $\langle \delta J(t)\ \delta J(t')\rangle = 2\gamma_1\hbar\ \delta(t\text{-}t')$. The Dirac δ-function $\delta(t\text{-}t')$ at the right-hand side of these expressions implies that the correlation time of the fluctuations is infinitely short. The parameters γ_0 and γ_1 are a measure for the strength of the fluctuations in the site energies and electronic couplings, respectively, and will depend on temperature. The exciton diffusion coefficient now becomes[29]

$$D = \frac{J^2a^2}{\hbar(\gamma_0 + 3\gamma_1)} + \frac{2\gamma_1 a^2}{\hbar} \tag{4}$$

The first term in eq 4 is the coherent part, which describes band motion that is hindered by fluctuations in the site energies and electronic couplings. The second term in eq 4 is solely due to fluctuations in the electronic couplings and is referred to as the incoherent part. The band motion of the exciton is thermally deactivated, since the magnitude of the fluctuations (and hence γ_0 and γ_1) will increase with temperature, causing a decrease of the first term in eq 4. Thermally deactivated band motion has been observed for excitons in crystals of naphthalene or anthracene molecules.[31,32] At higher temperatures the incoherent part of the diffusion coefficient in eq 4 may become dominant, giving rise to thermally activated exciton diffusion. Despite its approximate nature, eq 4 can be used for a qualitative discussion of effects of fluctuations in site energies and electronic couplings on exciton motion. More detailed theoretical models will yield similar trends (see ref 28 and references therein).

Insight into the mechanism of exciton motion can be obtained from the temperature dependence of the diffusion coefficient. Polaronic exciton motion (eq 2) gives rise to thermally activated diffusion, while band motion (first term in eq 4) is thermally deactivated. The present work involves a study of the effect of temperature on the exciton diffusion coefficient in a nematic TnBuPP layer. To the knowledge of the authors, the temperature dependence of the exciton diffusion coefficient in porphyrins has not been reported before. The exciton diffusion coefficient is found to decrease with temperature. Hence, exciton diffusion occurs via a band mechanism and is not limited by polaronic effects. This implies that the exciton diffusion coefficient in TnBuPP and related materials can be enhanced by reduction of structural fluctuations in the material.

II. Results and Discussion

Nematically organized layers of TnBuPP were prepared, as described in ref 21. The optical absorption and fluorescence characteristics were measured with equipment described in ref 33 using the methodology of ref 34. The temperature was varied from 90 to 300 K using an Oxford Optistat bath cryostat. Optical reflection spectra were measured at 300 K as described in ref 21 and assumed to be temperature independent. Figure 1A shows the optical absorption coefficient (α) and the fluorescence quantum yield (ϕ_F) of a 30 nm thick TnBuPP layer on quartz as a function of wavelength at 90 K (dashed) and 300 K (solid). The so-called Soret absorption band, which peaks at 436 nm, originates from the S_0-S_2 transition.[35] The full width at half-maximum (fwhm) of the Soret band increases slightly with temperature from 25 nm at 90 K to 29 nm at 300 K, coinciding with a small decrease of α. The transitions from the S_0 state to two energetically slightly different S_1 levels and their higher vibrational states lead to the four less intense Q-bands between 500 and 700 nm.[35] The decay from the lowest S_1 level toward the lowest vibrational state of the electronic ground-state gives rise to the most intense fluorescence band. The second fluorescence band is due to decay to a higher vibrational state of the electronic ground state.[35] Increasing the temperature results in a blue shift of the fluorescence bands and an enhancement of the intensity of the second fluorescence band. Figure 1B shows the time dependence of the fluorescence decay of TnBuPP on quartz at 90 and 300 K. The decay at 90 K clearly exhibits two different slopes. Fitting a biexponential function convoluted with the instrumental response function to this decay yields lifetimes of 0.52 and 2.7 ns, with the first component contributing the major part (87%) to the signal. At 300 K the fluorescence decay is slower than at 90 K and exhibits only one slope. Fitting a monoexponential function convoluted with the instrumental response function to this decay yields an exciton lifetime of

(29) Haken, H.; Reineker, P. *Z. Phys.* **1972**, *249*, 253–268.
(30) Haken, H.; Strobl, G. *Z. Phys.* **1973**, *262*, 135–148.
(31) Powell, R. C.; Soos, Z. G. *Phys. Rev. B* **1972**, *5*, 1547–1556.
(32) Ern, V.; Suna, A.; Tomkiewicz, Y.; Avakian, P.; Groff, R. P. *Phys. Rev. B* **1972**, *5*, 3222–3234.
(33) Gomez, R.; Veldman, D.; Blanco, R.; Seoane, C.; Segura, J. L.; Janssen, R. A. J. *Macromolecules* **2007**, *40*, 2760–2772.
(34) Kroeze, J. E.; Savenije, T. J.; Warman, J. M. *J. Am. Chem. Soc.* **2004**, *126*, 7608–7618.
(35) Gouterman, M., *The Porphyrins;* Academic Press: New York, 1978; Vol. 3.

1.95 ns.[36] Note, that these singlet exciton lifetimes are approximately 1 order of magnitude shorter than the time for intersystem crossing to the lowest triplet state.[37] Therefore, formation of triplet excitons can be ignored.

The effects of temperature on the optical characteristics of the TnBuPP layer can (in part) originate from slight changes in layer morphology with temperature; albeit that no phase transition was found from differential scanning calorimetry (DSC) measurements in the temperature range between 90 and 300 K. The enhancement of the exciton lifetime and the blue shift of the fluorescence at higher temperature could result from a decrease of the exciton diffusion length (as derived below), so that exciton relaxation at sites with a lower excitation energy or quenching at defects is reduced. This implies that the measured Stokes shift can to some extent be determined by spectral diffusion. The Stokes shift in Figure 1A is 60 ± 10 meV at 90 K and 15 ± 10 meV at 300 K. The latter value provides an upper limit to the value that would have to be invoked in eq 2 for the case of polaronic exciton hopping, since the exciton diffusion length is shortest at 300 K (see later), so that the contribution of spectral diffusion is smallest. The small value of the Stokes shift suggests that it is not likely that the exciton has a polaronic nature with a hopping rate described by eq 2, or an analogous expression obtained from quantum treatment of the relevant vibrations. Further insight into the mechanism of exciton motion is obtained from the effect of temperature on the exciton diffusion coefficient, as described below.

Exciton diffusion in the TnBuPP layer was studied using the time-resolved microwave conductivity (TRMC) method.[9,21,38,39] A layer of TnBuPP was deposited onto TiO_2 by spin-coating from chloroform. The sample was placed at maximum electric field strength in a temperature controlled X-band (8.2−12.4 GHz) microwave cavity (under N_2 atmosphere) and was irradiated via a grating in the cavity end-wall. The sample was illuminated using a Coherent Infinity laser, delivering pulses with a duration of 3.5 ns fwhm and tunable in a wavelength range of 410−700 nm and 240−320 nm. The incident intensity was varied between 1×10^{10} and 1×10^{12} photons/cm^2 per pulse, which was found to be sufficiently low, so that second order exciton annihilation or charge recombination processes are insignificant. Photoexcitation of the TnBuPP layer at 430 nm (close to the maximum of the Soret absorption band) leads to the production of excitons (process 1 in Figure 2). The excitons can decay (non)radiatively to the ground state or they can reach the interface with TiO_2 by diffusion through the TnBuPP layer (process 2 in Figure 2). At the interface an exciton can dissociate into separate charge carriers by electron injection into TiO_2 (process 3 in Figure 2), leading to the formation of highly mobile conduction band electrons in the TiO_2 layer. These electrons give rise to a change in microwave power reflected by the cavity, from which the increase in photoconductance, $\Delta G(t)$, can be determined. Eventual trapping and recombination of the mobile electrons leads to decay of $\Delta G(t)$.

The exciton diffusion length can be determined from the ratio of the number of electrons injected into TiO_2 to the number of incident photons; that is, the incident photon to charge separation efficiency (IPCSE). The IPCSE was determined by normalization of $\Delta G(t)$ on excitation with 430 nm to the maximum value of the transient photoconductance obtained on selective excitation of the TiO_2 layer at 300 nm ($\Delta G_{\max,\lambda=300\text{nm}}$), as described in ref 39. In this way the effect of the temperature dependence of the electron mobility in TiO_2 on $\Delta G(t)$ at 430 nm excitation is taken into account. The value of the IPCSE depends on the efficiency of processes 1−3 in Figure 2, according to[39]

$$\text{IPCSE} = (1 - F_R)\varphi_{gen}\, S(\alpha, \Lambda_E, L)\ 100\% \qquad (5)$$

where F_R is the fraction of photons reflected at the sample surface and ϕ_{gen} is the interfacial charge generation yield relative to all modes of interfacial exciton deactivation. The factor S represents the number of excitons that reaches the interface between TnBuPP and TiO_2 normalized to $I_0(1 - F_R)$; that is, the number of photons entering the sample. Analytical expressions for S are given in the Supporting Information. The factor S depends on the optical absorption coefficient (α), the value of Λ_E, the thickness of the TnBuPP layer (L), and the side from which the laser pulse enters the sample; that is, the side of the TiO_2 substrate or the side of the TnBuPP layer.

The effect of temperature on ϕ_{gen} was determined from the experimental IPCSE value for a thin layer of 0.75 nm TnBuPP on TiO_2, see Figure 2A. In this thin layer almost all TnBuPP molecules are in direct contact with TiO_2. Hence, dissociation of excitons at the interface between TnBuPP and TiO_2 is not limited by diffusion and the factor S in eq 5 equals the fraction of the incident photons that is absorbed in the TnBuPP layer, see Supporting Information. Figure 2C shows the normalized photoconductance transients at 90 K (dashed) and 300 K (solid) obtained on pulsed excitation of the 0.75 nm TnBuPP layer at 430 nm. The sample was photoexcited from the side of the TiO_2 substrate. The initial rise of the transients is due to the 18 ns instrument response time of the system. After having reached a maximum, the transient photoconductance decreases slowly due to decay of charges. The maximum value in the transient of $\Delta G(t)/\Delta G_{\max,\lambda=300\text{nm}}$ at 300 K significantly exceeds that at 90 K. Using the methodology described in ref , the IPCSE value for the 0.75 nm TnBuPP layer is determined to be 0.2% at 90 K and 0.8% at 300 K. The initial number of excitons produced in TnBuPP at 90 K is almost identical to that at 300 K, since the optical absorption coefficient is hardly temperature dependent, see Figure 1A. The enhancement of the IPCSE from 0.2% to 0.8% on increasing the temperature must thus be due to a 4-fold increase of ϕ_{gen}, see eq 5. The increase of ϕ_{gen} with temperature likely originates from a larger yield of escape of electrons and holes from interfacial charge recombination at higher temperatures. Also, the geometry of a TnBuPP cation will differ to some extent from a neutral excited TnBuPP molecule. It then follows from the Marcus theory for electron transfer,[26,40] that the rate of electron injection in TiO_2, and in turn ϕ_{gen}, can become thermally activated.

The effect of temperature on the exciton diffusion coefficient, or equivalently on the factor S in eq 5, was determined from photoconductance measurements on the 30 nm thick TnBuPP layer on TiO_2, see Figure 2B. The sample was photoexcited from the side of the TiO_2 substrate. The IPCSE obtained from the photoconductance transients in Figure 2D increases with

(36) This value exceeds the exciton lifetime of 1 ns reported in ref 21. The difference originates from the fact that the experiment in ref 21 involves a freshly prepared sample for which the exciton lifetime has not reached the steady-state value of 2 ns, while the current lifetime has been determined for a sample for which the exciton lifetime has stabilized to 1.95 ns at 300 K.

(37) Kalyanasundaram, K.; Neumann-Spallart, M. *J. Phys. Chem.* **1982**, *86*, 5163–5169.
(38) de Haas, M. P.; Warman, J. M. *Chem. Phys.* **1982**, *73*, 35–53.
(39) Kroeze, J. E.; Savenije, T. J.; Vermeulen, M. J. W.; Warman, J. M. *J. Phys. Chem. B* **2003**, *107*, 7696–7705.
(40) Marcus, R. A. *Rev. Mod. Phys.* **1993**, *65*, 599–610.

temperature from 8% at 90 K to 20% at 300 K. The latter value agrees with previous experiments.[21] In earlier measurements the value of ϕ_{gen} was found to be independent of the porphyrin layer thickness.[41] Since the enhancement of the IPCSE on going from 90 to 300 K is less than the 4-fold increase of ϕ_{gen}, it can be concluded that the factor S decreases with temperature, see eq 5. This could either originate from a decrease of α or from a reduced Λ_E. The only weak temperature dependence of α (see Figure 1A) excludes the first option and leads to the conclusion that the value of Λ_E has to decrease on increasing the temperature. The value of Λ_E decreases with increasing temperature, despite the fact that τ_E is longer at higher temperature. This implies that the exciton diffusion coefficient, D_E, decreases with temperature, see eq 1. Hence, exciton diffusion in TnBuPP is thermally deactivated.

The values of ϕ_{gen} and Λ_E were determined from the dependence of the IPCSE on the TnBuPP layer thickness L (see data in Supporting Information), as described previously.[41] It was found that $\phi_{gen} = 0.60 \pm 0.05$ and $\Lambda_E = 22 \pm 3$ nm at 300 K. According to eq 1 this value for Λ_E together with the exciton lifetime of 1.95 ns yields $D_E = (2.5 \pm 0.5) \times 10^{-7}$ m^2/s at 300 K. The 4-fold decrease in ϕ_{gen} on reducing the temperature leads to $\phi_{gen} = 0.15 \pm 0.01$ at 90 K. This value and the IPCSE value of 8% for the 30 nm thick TnBuPP layer gives $\Lambda_E \geq 40$ nm at 90 K. Combining this with the exciton lifetime of 0.52 ns leads to $D_E \geq 3.1 \times 10^{-6}$ m^2/s at 90 K. Only a lower limit to Λ_E can be determined at 90 K, since the exciton diffusion length exceeds the maximum thickness (35 nm) for which a TnBuPP layer with nematic organization as depicted in Figure 2B could be prepared, see Supporting Information.

The exciton diffusion coefficient decreases by at least 1 order of magnitude on increasing the temperature from 90 to 300 K. This leads to the conclusion that excitons in TnBuPP are not of polaronic nature and their motion cannot be described on the basis of eq 2, as already suggested by the small Stokes shift as discussed above. Even for a vanishing value of E_s in eq 2 the diffusion constant would weakly decrease with temperature according to the $T^{-1/2}$ factor. This would result in a reduction of the diffusion coefficient by only a factor two on going from 90 to 300 K, in disagreement with the experimental results. In addition, the assumption of a vanishing value of E_s, would imply that the exciton does not have a polaronic nature, which is in conflict with using eq 2. The occurrence of a larger value of E_s in eq 2, or inclusion of effects of static disorder in the site energies would lead to an even lower decrease of the exciton diffusion coefficient with temperature, or, more likely, to thermally activated diffusion. The observed strong decrease of the exciton diffusion coefficient with temperature can be understood on the basis of band motion of the exciton, as described by the first term in eq 4. Increasing the temperature enhances the structural fluctuations in the material. This leads to an increase of the fluctuations in the exciton site energies and electronic couplings (i.e. the parameters γ_0 and $\gamma_1$in eq 4) and in turn to a decrease of the exciton diffusion coefficient for band motion (first term in eq 4). Apparently, the incoherent part of the diffusion coefficient (second term in eq 4) is not dominant at the temperatures considered, since this would lead to thermally activated exciton diffusion. It is therefore inferred that exciton motion in a TnBuPP layer occurs via a thermally deactivated band mechanism.

(41) Huijser, A.; Savenije, T. J.; Kroeze, J. E.; Siebbeles, L. D. A. *J. Phys. Chem. B* **2005**, *109*, 20166–20173.

III. Conclusion

Exciton diffusion in a nematically organized TnBuPP layer occurs over a distance as long as tens of nanometers. The exciton diffusion coefficient decreases by at least an order of magnitude on increasing the temperature from 90 to 300 K. This can be ascribed to enhanced structural fluctuations at higher temperature and in turn larger fluctuations in the exciton site energies and electronic couplings for energy transfer from one molecule to another. The thermal deactivation of the exciton diffusion coefficient indicates that exciton diffusion in a TnBuPP layer occurs via a nonpolaronic band mechanism. The magnitude of the exciton diffusion coefficient is not limited by the induction of a lattice deformation around the exciton. The absence of such self-induced trapping implies that the exciton diffusion coefficient can be enhanced by reduction of structural fluctuations.

A similar band mechanism for exciton motion is also expected for other molecular materials with a large aromatic core. In such molecules electrons are delocalized over the large aromatic core both in the ground-state and in the excited state. Photoexcitation of an electron does not significantly alter the charge distribution within the molecule. Consequently, the nuclear geometry of the molecule in the ground-state and the excited-state will be similar and polaronic self-trapping of the exciton will be insignificant. Exciton motion then occurs via a band mechanism, as discussed above.

Acknowledgment. This research is supported financially by the Delft Research Centre for Sustainable Energy.

Supporting Information Available: Derivation of analytical expressions for the factor S in eq 5. Measured IPCSE values for various thicknesses of the TnBuPP layer. This material is available free of charge via the Internet at http://pubs.acs.org.

JA803753Y